

SYNTHESIS AND CHARACTERIZATION OF CELLULOSE AND CELLULOSE NANOCRYSTALS FROM DEAD SEAGRASS – TOWARDS THE WEALTH FROM WASTE CONCEPT

RAHUL VARMA and SUGUMAR VASUDEVAN

*Department of Oceanography and Coastal Area Studies, Alagappa University,
Science Campus, Karaikudi 630 003, Tamil Nadu, India*

✉ *Corresponding author: S. Vasudevan, crustacealab@gmail.com, sugumarv@alagappauniversity.ac.in*

Received September 8, 2021

The study has demonstrated that decaying seagrass accumulated along the shores is a particularly good source of cellulose and cellulose nanocrystals (CNCs). The FTIR spectra indicated the presence of O-H and C-H bonds in both the cellulose and CNCs obtained from the seagrass biomass. The Micro-Raman spectra showed maximum peaks at 1277 cm^{-1} for cellulose and at 1108 cm^{-1} for CNCs. The XRD spectra of cellulose confirmed its crystallinity, with a maximum peak for both cellulose and CNCs at 22° . The thermal stability of cellulose was lower than that of CNCs, where the latter showed thermal stability ranging between $110\text{-}250\text{ }^\circ\text{C}$. Overall, the cellulose and CNCs obtained showed good crystallinity and thermal stability. The particle size of the CNCs was recorded to be 253.2 nm . Also, they have a large surface area to volume ratio, which contributes to their high strength and stiffness. Thus, the cellulose and CNCs produced from decaying seagrass impart economic value to waste biomass, which can be a step towards the implementation of the wealth from the waste concept.

Keywords: cellulose, cellulose nanocrystals, characterization, biopolymer, seagrass

INTRODUCTION

Seagrasses are a polyphyletic angiosperm plant group that developed from early monocotyledonous land plants and returned to the sea roughly 140 million years ago.¹ Large seagrass beds are one of the world's most significant ecosystems, and they are crucial from an ecological standpoint since they provide a home for microinvertebrates.² Knowing the composition of polysaccharides in fibrous seagrass can help researchers better understand the long-term stability of distinct polysaccharide groups.² The major component of seagrass cell walls is cellulose, being similar to angiosperm terrestrial plants. The content of cellulose in different genera has been evaluated related to dry plant material.¹ In recent years, certain studies have emphasized the usefulness of dead seagrass material as an ecological or coast-protecting resource.² With these considerations, this paper focuses on the molecular characterisation of cellulose and cellulose nanocrystals in dead seagrass material to provide solutions for seagrass waste reuse.

Cellulose is one of the most widely found biopolymers on the earth, which has found a wide variety of applications, including in food packaging, innovative green composites and paper-making.³ The extraction and application of cellulose has a great impact on the sustainable development of human society.⁴ The strength and resistance of this polymer to degradation are due to the stiff and ordered structures of its microfibrils.⁵ Cellulose is composed of straight chains of D-glucose connected by β -1,4-glycosidic linkages, with a high-quality form of polymerization of 1×10^3 in native woods.⁶

Cellulose as a crystalline polymer is characterized by its polymorphism, *i.e.* its ability to form crystallites with various unit cell properties. Currently, six polymorphic modifications of cellulose are known. In cellulose samples obtained from primitive organisms (bacteria, algae), the low-symmetric phase Ia predominates, while in higher plants the I β form is prevalent.⁷

Cellulose nanocrystals (CNCs) are unique nanomaterials that are derived from cellulose mainly by acid hydrolysis.⁹ Due to their exceptional features, including high mechanical, barrier, optical, rheological and non-toxicity properties,⁸ in recent years, cellulose nanocrystals (CNCs) have gained huge importance in a variety of different fields. The high mechanical strength and the large surface area of cellulose nanocrystals recommend them as an additive for the consolidation of hybrid nanocomposite systems. Their application in the biomedical, pharmaceutical and food packaging areas has been increasing steadily due to their interface stabilizing ability, chemical inertness and non-toxicity.¹⁰ Cellulose nanocrystals are known to show explicit optical and liquid crystalline properties, and nanoparticle-coated cellulose paper has been reported in the usage of water purification.¹¹ The morphology of cellulose nanocrystals is known to affect the distribution of particles. Similarly, the crystallinity of the nanomaterial has an important influence on the physical properties of the cellulose nanocrystals.¹² Normally, cellulose nanocrystals are known to possess high crystallinity. Their increased crystallinity is possible due to hydrolysis using acids, which destroy the amorphous regions in the structure, eventually leaving only the crystalline zone in the structure.^{13–15}

The applications cellulose and of cellulose nanocrystals are highly dependent upon the choice of the biomass source and the chemical treatment used for their extraction. Therefore, the characterization of the isolated materials through FTIR,¹⁶ Micro-Raman spectroscopy, XRD¹⁷ and other techniques is essential. Thus, in FTIR, for example, the peak found approximately around 1734 cm^{-1} is generally attributed to the C=O stretching of the acetyl and uronic ester groups of polysaccharides, and is also related to the p-coumaric acids of lignin and/or hemicellulose, therefore its disappearance in the treated material indicates the removal of most of lignin and hemicelluloses.¹⁶ In the Micro-Raman spectrum of cellulose, the shifts of the 1095 cm^{-1} band provide information on the molecular deformation of the material, which is related to the stress within the fibre. However, although the Raman frequency, intensity, and band shape of the vibrations can vary between the celluloses and nanocellulose, nanocellulose does not have distinctive Raman spectra, and therefore this

technique cannot be used alone to prove the existence of nanocellulose.

The studies regarding the thermal stability of nanocellulose are very important for its utilization in applications such as food packaging material.⁸ It has been suggested that the thermal stability of the CNCs reduces with an increase in the acid hydrolysis temperature and time.¹⁸ Some studies have also shown that the thermal stability of cellulose varies with its source.¹⁹ According to other research, the time taken for acid hydrolysis and the duration of sonication have a significant impact on the particle size of CNCs.²⁰ The acid concentration employed also impacts particle size, since a larger concentration permits deeper penetration of the acid and causes increased fragmentation, resulting in the production of CNCs with smaller diameters.²¹

Considering that, due to their properties, nanocellulose materials have gained much interest from researchers and industries alike, the present work aims to extract cellulose nanocrystals from dead and decaying seagrass as a way to impart value to a biomass waste. The extracted cellulose and CNCs were then characterized by FTIR, Micro-Raman spectroscopy, XRD, TGA and particle size analysis.

EXPERIMENTAL

Sample collection

As dead seagrass is abundantly deposited by tidal currents on the coast of Thondi (9.74° N and 79.01° E), samples were collected directly from the shore. The collected samples were thoroughly dried under the sun for several days, until completely dry, and suitable for further processing.

Extraction of cellulose

Cellulose was extracted from the dead seagrass samples following the methodology proposed by Szymanska-Chargot *et al.*,⁵ with slight modification. The seagrass samples were firstly dried and pulverized. The sample was then allowed to boil in water for 10 minutes. The boiling of the sample removes sugar, phenolic compounds and polysaccharides, which are water-soluble. Later, the residue obtained was used for acid hydrolysis using 1M hydrochloric acid. The sample (30 g) was treated with 100 mL of 1M hydrochloric acid at 85° C for 30 minutes. This step was repeated, so that the maximum quantity of pectic polysaccharides could be removed. The next step was alkaline hydrolysis using 1M sodium hydroxide. The sample was allowed to react with 1M sodium hydroxide for half an hour at 85° C . This step removes hemicelluloses; it was carried out thrice to ensure their complete removal. The final step for the extraction of

cellulose was a bleaching process, where the sample was treated with 1-2% sodium hypochlorite for one hour at 95 °C. The bleaching process was repeated twice, and the precipitate obtained was cellulose. The cellulose obtained was washed multiple times with running water until a neutral pH was reached.

Extraction of cellulose nanocrystals (CNCs)

The extraction of cellulose nanocrystals was achieved through acid hydrolysis by the method proposed by Sai Prasanna and Mitra,⁸ with slight modification. The cellulose obtained, 5 g, was allowed to react with 100 mL of 55 wt% H₂SO₄, under continuous stirring at 45 °C for 30 minutes. After this time, the reaction was quenched by the addition of 1 L of distilled water. The precipitate formed was centrifuged at 10000 rpm for 10 minutes, and the pH of the solution was brought up to neutral by continuous centrifugation and by dialysis in water. The precipitate was then subjected to sonication at 225 W for 10 minutes. The suspension obtained represented cellulose nanocrystals and was stored at 4 °C for further analysis.

Characterization of cellulose and cellulose nanocrystals

Fourier transform infrared spectroscopy

The cellulose and cellulose nanocrystals were subjected to KBr assisted FTIR analysis, using a Perkins-Elmer spectrometer (Spectrum Rx1, MA, USA). The FTIR spectra were recorded at a resolution of 4 cm⁻¹ in the frequency range of 4000-400 cm⁻¹.

Micro-Raman spectroscopy

In the present investigation, micro-Raman spectra were used to study the vibrational modes of the obtained cellulose and CNCs using a Princeton Acton SP 2500 instrument (Japan) under an excitation wavelength of 632 nm with an argon laser.

X-ray powder diffraction

The crystalline nature of the cellulose nanocrystals was detected by using X'pert ProPanAnalytical equipment (the Netherlands). The instrument was operated at 40 kV and 30 mA with Cu K α = 1.5406 Å.

Thermogravimetric analysis

Thermal analysis of the cellulose and CNCs samples was performed with the help of a Mettler Toledo TGA 2, in the temperature range from 50 to 600 °C.

Particle size analysis

The particle size of the cellulose nanocrystals was measured using NanoPlus Dynamic Light Scattering (DLS) (Micromeritics) equipment. The CNC samples were dispersed in water and then subjected to sonication in an ultrasonic water bath for 5 minutes,

before being introduced into the particle size analyzer. The analysis was run at a temperature of 25 °C.

RESULTS AND DISCUSSION

The raw dead seagrass material collected from the coast of Thondi weighed about 30 g. The amount of cellulose extracted from 30 g of raw material was calculated to be 10 g, and the amount of cellulose nanocrystals extracted from 10 g of cellulose was calculated to be 1.706 g. The percentage of yield of cellulose from 100 g of raw material was calculated to be 33.3%, while the percentage yield of CNCs from cellulose was calculated to be 17.06%. Previous studies revealed percentage yields of cellulose and CNCs in the ranges of 12%-25% and 30%-40%, respectively.²²⁻²⁵

Fourier transform infrared spectroscopy

The FTIR spectra of cellulose and CNCs extracted from dead seagrass are given in Figures 1 and 2, respectively. The absorption bands in the spectrum of cellulose are observed in the wavenumber regions of 3600-2500 cm⁻¹ and 1700-400 cm⁻¹. The major peaks are located at 3353 cm⁻¹, 2890 cm⁻¹, 1328 cm⁻¹, 1314 cm⁻¹ and 889 cm⁻¹. In the case of cellulose nanocrystals, the absorption bands are observed between 3500-3000 cm⁻¹ and 2200-500 cm⁻¹ (Fig. 2). The major peaks in the case of cellulose nanocrystals were observed at the wavenumbers 3336 cm⁻¹, 1637 cm⁻¹, 1433 cm⁻¹, 1320 cm⁻¹ and 1049 cm⁻¹.

The peaks in the wavenumber region 3600-2500 cm⁻¹ is characteristic of the stretching vibration of O-H and C-H bonds in cellulose. The peak located at 3353 cm⁻¹ denotes the stretching vibration of the hydroxyl group and represents the intramolecular and intermolecular hydrogen bonding vibrations in the polysaccharides.²³ The peak seen at the wavenumber 1328 cm⁻¹ may be attributed to the C-H bending vibration and the one noted at 1314 cm⁻¹ represents CH₂ wagging.²⁶⁻²⁸ The peak present at the wavenumber 889 cm⁻¹ represents the OH bending in the cellulose.²⁶

In the cellulose nanocrystals, the peak found at 3336 cm⁻¹ is associated with the stretching of OH groups and represents inter- and intramolecular hydrogen bonds.²⁹ This peak also demonstrates the hydrophilic nature of the CNCs. The peak present at 1433 cm⁻¹ is associated with the asymmetric stretching vibration of carboxylate groups (C=O), while the peak at 1049 cm⁻¹ represents the C-O stretching vibration.²⁴ The O-

H bending vibration of adsorbed water was found to be present at the peak of 1637 cm^{-1} .¹⁹ The bending vibrations and angular deformation of the C–H and C–O groups were represented by the peak at 1320 cm^{-1} , which corresponds to the polysaccharide aromatic ring.¹⁹ The asymmetric $\text{C}_1\text{--O--C}_4$ linkage was represented by the peak at 1156 cm^{-1} , whereas the carbohydrate rings were represented by the peak at 1049 cm^{-1} .²⁹ In the cellulose structure, the peak at 1433 cm^{-1} represented the symmetric CH_2 structure. C–H bonds in polysaccharide rings are shown by the peak at 1320 cm^{-1} . The O–H bonding of the

adsorbed water was ascribed to the peak at 1637 cm^{-1} .³⁰

Micro-Raman spectroscopy

The micro-Raman spectra of the cellulose and CNCs extracted from dead seagrass are given in Figures 3 and 4, respectively. The spectra range between 300 cm^{-1} and 1800 cm^{-1} . The characteristic bands of cellulose are observed at the wavenumbers of 462 cm^{-1} , 1080 cm^{-1} , 1130 cm^{-1} and 1277 cm^{-1} . In the case of the cellulose nanocrystals, the major peaks were found at the wavenumbers of 340 cm^{-1} , 616 cm^{-1} , 1034 cm^{-1} and 1108 cm^{-1} (Fig. 4).

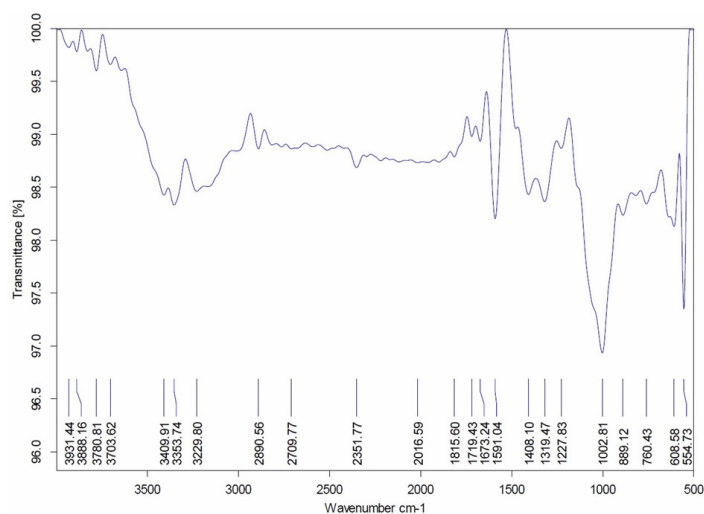


Figure 1: FTIR spectrum of cellulose extracted from decaying seagrass

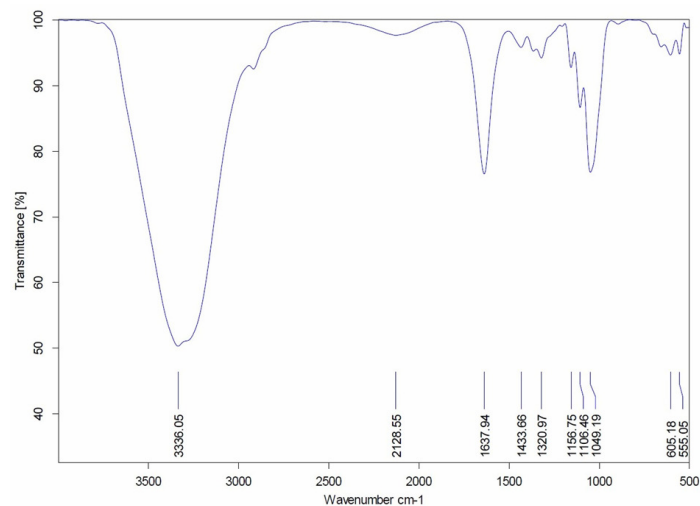


Figure 2: FTIR spectrum of CNCs extracted from decaying seagrass

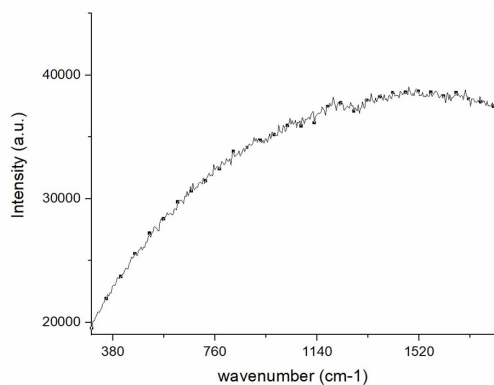


Figure 3: Micro-Raman spectrum of cellulose extracted from decaying seagrass

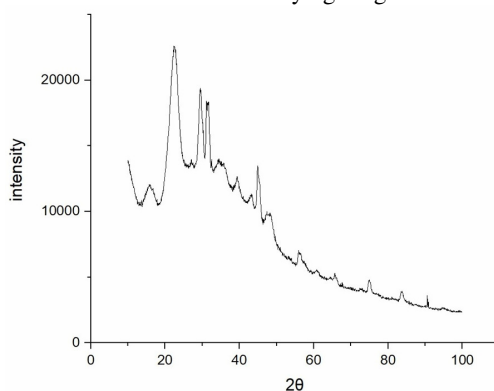


Figure 5: XRD pattern of cellulose extracted from decaying seagrass

The peak observed at 462 cm^{-1} represents the deformation of COC and CCC rings, while the peak located at 1080 cm^{-1} shows the COC symmetric stretching of the glycosidic ring. Similarly, the peaks identified at 1130 cm^{-1} and 1290 cm^{-1} represent the COC asymmetric stretching and CH_2 bending, respectively.^{31,32} In the case of cellulose nanocrystals, the peaks found at the wavelength of 340 cm^{-1} are attributed to the presence of heavy atom bending, while the peak at the wavelength of 616 cm^{-1} denotes the presence of the acetyl group. The peak found at 1034 cm^{-1} is assigned to the stretching of CC and CO bonds, while the peak obtained at 1290 cm^{-1} shows the presence of HCC and HCO bending.^{33,34}

X-ray powder diffraction (XRD)

The XRD pattern of cellulose shows peaks at $2\theta = 22^\circ, 29^\circ, 31^\circ$ and 44° (Fig. 5). Most of the previous studies report the maximum peak for cellulose to be at $2\theta = 22^\circ$.^{17,32} The peak observed at $2\theta = 22^\circ$ shows the typical structure of

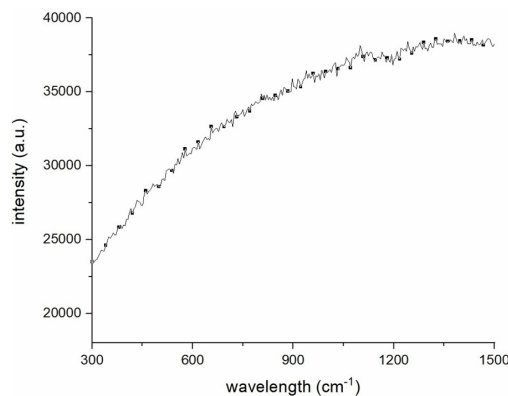


Figure 4: Micro-Raman spectrum of CNCs extracted from decaying seagrass

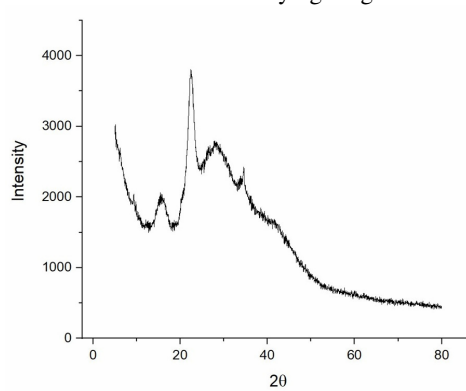


Figure 6: XRD pattern of CNCs extracted from decaying seagrass

cellulose, indicating its crystallinity. This result is in agreement with those of previous studies.^{35,36}

The X-ray powder diffraction pattern of the cellulose nanocrystals reveals peaks at $2\theta = 15^\circ, 27^\circ$ and 34° , and the maximum peak is observed at 22° (Fig. 6). The maximum peaks of both the cellulose and CNCs are found to be the same, which has been also confirmed in previous studies.³⁷ The results obtained in this work suggest that there was no variation in the structural characteristics of cellulose, even after the acid hydrolysis and purification processes.³⁸ The peaks found in this study are generally attributed to the cellulose I type structure, and there was no discernible variation in the pattern of the detected peaks for the CNCs.³⁹ It meant that no polymorphs from the original cellulose I had been converted to cellulose II in the nanocrystals.⁴⁰

Thermogravimetric analysis (TGA)

The thermal stability of both the cellulose and cellulose nanocrystals was analysed in the range

from 50 to 600 °C. Figure 7 displays the thermogram of cellulose, which reveals a 9.21% decrease in the mass of cellulose in the first stage between 50-100 °C. The second stage shows a loss of mass of 40.76% between 250-350 °C. The complete decomposition of cellulose was observed at 410-490 °C. The first stage of mass loss is attributed to dehydration of the sample, while the second one is caused by the degradation of cellulose. The results obtained showed similarities to those of previous studies.^{6,25}

In the case of cellulose nanocrystals, the thermogram recorded in the range from 50 to 600 °C (Fig. 8) shows a 69.80% loss of mass in the first stage, between 50-100 °C, and another mass loss of 21.01% was noted in the second stage, between 110-330 °C. The third stage of

degradation was observed between 340-450 °C, with a loss of mass of 4.72%. The initial mass loss was caused by the evaporation of water, while the second was attributed to the depolymerization of cellulose. The final mass loss can be explained by the depolymerization of carbon residues. It has been reported that the thermal characteristics of cellulose nanocrystals vary greatly, and it was shown that lower crystallinity, greater sulphur content, and smaller cellulose crystallite size can speed up thermal disintegration and impair thermal durability.⁴⁴ In our study, the cellulose nanocrystal sample did not show any decomposition in the range of 110-250 °C, which shows its thermal stability. These results agree with previous studies.⁴¹⁻⁴³

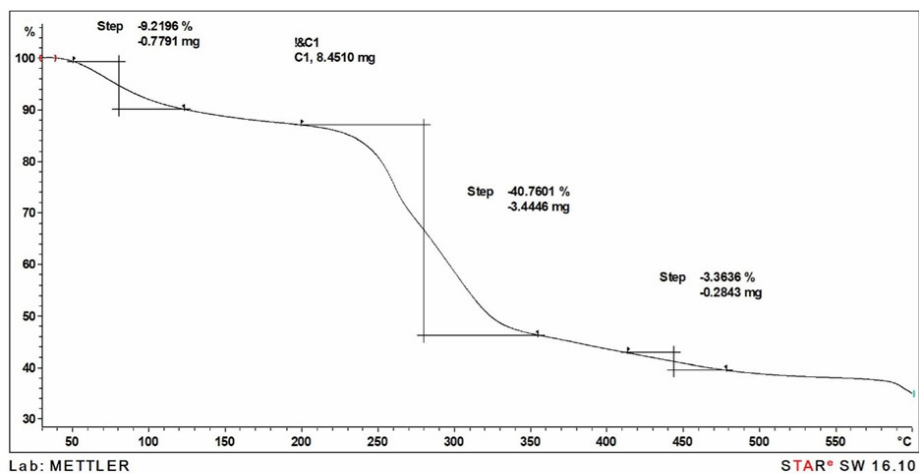


Figure 7: TGA thermogram of cellulose extracted from decaying seagrass

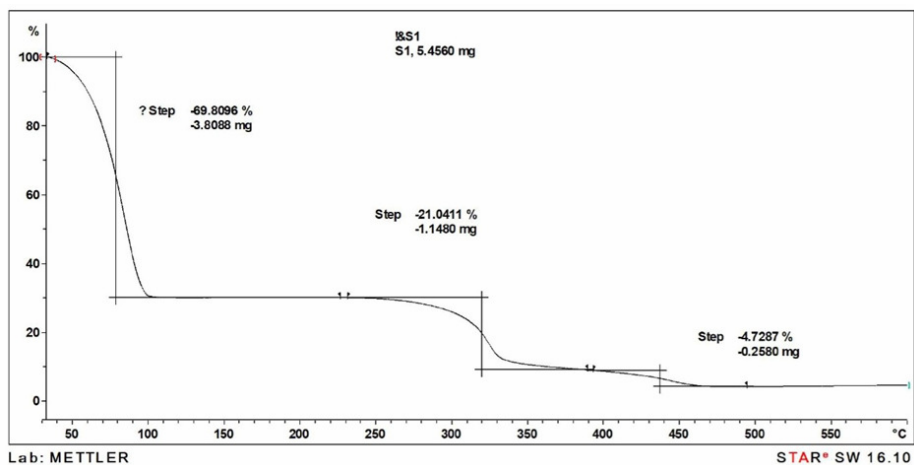


Figure 8: TGA thermogram of CNCs extracted from decaying seagrass

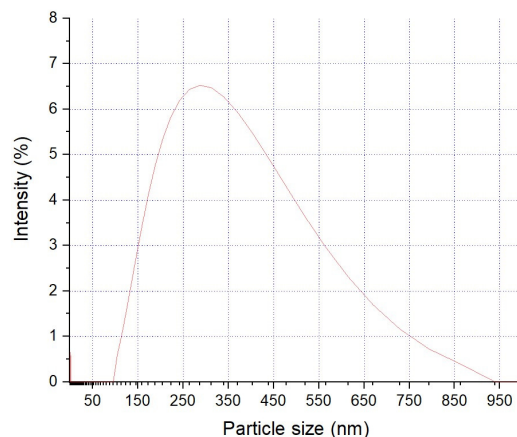


Figure 9: Particle size analysis of CNCs from decaying seagrass

Particle size analysis

The particle size distribution of the cellulose nanocrystals is illustrated in Figure 9. The results obtained showed a single peak, with a diameter of 253.2 nm, and this indicates the average size of the CNCs. The obtained results are similar to the results obtained by Pandi *et al.*, and Meyabadi *et al.*^{45,46} The study conducted by Pandi *et al.*⁴⁵ reported the size of CNCs to be in the range of 100 and 800 nm, while Meyabadi *et al.*⁴⁶ obtained CNCs with particle sizes in the range of 100 and 300 nm. The particle size obtained in the present work is well within the ranges reported previously. Different diameter and length values for rod-shaped nanocrystals have been reported by researchers, including 207.2 nm in length and 23.2 nm for diameter,⁴⁷ 87 nm in length and 12 nm in diameter,⁴⁸ or 135 nm in length and 7.2 nm in diameter.⁴⁹ The length values revealed by DLS analysis are similar to these. Therefore the results of DLS analysis confirmed that the cellulose particles isolated from dead seagrass are mostly nanometric in size.

CONCLUSION

Dead and decaying seagrass is commonly found deposited by tidal waves on the coast of Thondi. The present study showed that this type of waste biomass can be a good source of cellulose, as well as of cellulose nanocrystals. The extracted cellulose and CNCs were subjected to various characterization studies, using Fourier transform infrared spectroscopy (FTIR), micro-Raman spectroscopy, X-ray powder diffraction (XRD), thermogravimetric analysis (TGA) and particle size analysis. The FTIR and micro-Raman analysis confirmed the chemical bonds present in the sample, while the XRD study displayed the

crystalline nature of the extracted cellulose and cellulose nanocrystals. The TGA of the cellulose and cellulose nanocrystals revealed better thermal stability of the CNCs, compared to that of cellulose. The particle size analysis of the extracted CNCs confirmed that their size falls under the required nanoscale. The results obtained in this work have been confirmed by the findings of previous literature reports. Future research on cellulose and CNCs from dead and decaying seagrass will focus on the suitability of these materials for producing thin films and their application in food packaging products.

ACKNOWLEDGEMENT: We gratefully acknowledge the funding received from the RUSA-Phase 2.0 grant No. F24-51/2014-U, Policy (TN Multi-Gen), (09.10.2018), Department of Education, Govt. of India.

REFERENCES

- 1 L. Pfeifer and B. Classen, *Front. Plant Sci.*, **11**, 1 (2020), <https://doi.org/10.3389/fpls.2020.588754>
- 2 L. Pfeifer, *Polymers (Basel)*, **13**, 4285 (2021), <https://doi.org/10.3390/polym13244285>
- 3 S. Singh, K. K. Gaikwad, S. Il Park and Y. S. Lee, *Int. J. Biol. Macromol.*, **99**, 506 (2017), <http://dx.doi.org/10.1016/j.ijbiomac.2017.03.004>
- 4 H. Xie, H. Du, X. Yang and C. Si, *Int. J. Polym. Sci.*, **2018**, 7923068 (2018), <https://doi.org/10.1155/2018/7923068>
- 5 M. Szymanska-Chargot, M. Chylinska, K. Gdula, A. Koziol and A. Zdunek, *Polymers (Basel)*, **9**, 495 (2017), <https://doi.org/10.3390/polym9100495>
- 6 N. Rehman, S. Alam, N. U. Amin, I. Mian and H. Ullah, *Int. J. Polym. Sci.*, **2018**, 8381501 (2018), <https://doi.org/10.1155/2018/8381501>
- 7 K. Bogolitsyn, A. Parshina and L. Aleshina, *Cellulose*, **27**, 9787 (2020), <https://doi.org/10.1007/s10570-020-03485-z>

- ⁸ N. Sai Prasanna and J. Mitra, *Carbohydr. Polym.*, **247**, 116706 (2020), <https://doi.org/10.1016/j.carbpol.2020.116706>
- ⁹ M. Martelli-Tosi, M. D. S. Torricillas, M. A. Martins, O. B. G. De Assis and D. R. Tapia-Blácido, *J. Nanomater.*, **2016**, 8106814 (2016), <https://doi.org/10.1155/2016/8106814>
- ¹⁰ N. O. Okamoto-Schalch, S. G. B. Pinho, T. T. de Barros-Alexandrino, G. C. Dacanal, O. B. G. Assis *et al.*, *Cellulose*, **27**, 5855 (2020), <https://doi.org/10.1007/s10570-020-03173-y>
- ¹¹ W. Chen, F. Chen, G. Zhang, X. Liu, S. Kong *et al.*, *Cellulose*, **26**, 7027 (2019), <https://doi.org/10.1007/s10570-019-02620-9>
- ¹² U. P. Agarwal, R. S. Reiner, S. A. Ralph, J. Catchmark, K. Chi *et al.*, *Cellulose*, **28**, 1369 (2021), <https://doi.org/10.1007/s10570-020-03590-z>
- ¹³ R. A. Ilyas, S. M. Sapuan, M. R. Ishak and E. S. Zainudin, *Carbohydr. Polym.*, **202**, 186 (2018), <https://doi.org/10.1016/j.carbpol.2018.09.002>
- ¹⁴ G. Mondragon, S. Fernandes, A. Retegi, C. Peña, I. Algar *et al.*, *Ind. Crop. Prod.*, **55**, 140 (2014), <https://doi.org/10.1016/j.indcrop.2014.02.014>
- ¹⁵ A. Kaushik, M. Singh and G. Verma, *Carbohydr. Polym.*, **82**, 337 (2010), <http://dx.doi.org/10.1016/j.carbpol.2010.04.063>
- ¹⁶ A. Khenblouche, D. Bechki, M. Gouamid, K. Charradi, L. Segni *et al.*, *Polimeros*, **29**, 1 (2019), <https://doi.org/10.1590/0104-1428.05218>
- ¹⁷ A. Moradbak, P. M. Tahir, A. Z. Mohamed, M. M. Abdi, R. L. Razalli *et al.*, *Eur. J. Wood Wood Prod.*, **76**, 1021 (2018), <http://dx.doi.org/10.1007/s00107-017-1244-1>
- ¹⁸ Kusmono, R. F. Listyanda, M. W. Wildan and M. N. Iman, *Heliyon*, **6**, e05486 (2020), <https://doi.org/10.1016/j.heliyon.2020.e05486>
- ¹⁹ R. Radakisnin, M. S. A. Majid, M. R. M. Jamir, M. Jawaid, M. T. H. Sultan *et al.*, *Materials (Basel)*, **13**, 4125 (2020), <https://doi.org/10.3390/ma13184125>
- ²⁰ T. Sultana, S. Sultana, H. P. Nur and M. W. Khan, *J. Compos. Sci.*, **4**, 1 (2020), <https://doi.org/10.3390/jcs4030083>
- ²¹ C. P. Chang, I. C. Wang, K. J. Hung and Y. S. Perng, *Taiwan J. For. Sci.*, **25**, 251 (2010), <https://doi.org/10.7075/TJFS.201009.0251>
- ²² Y. Zhao and J. Li, *Cellulose*, **21**, 3427 (2014), <https://doi.org/10.1007/s10570-014-0348-6>
- ²³ Q. Q. Wang, J. Y. Zhu, R. S. Reiner, S. P. Verrill, U. Baxa *et al.*, *Cellulose*, **19**, 2033 (2012), <https://doi.org/10.1007/s10570-012-9765-6>
- ²⁴ M. El Achaby, N. El Miri, A. Aboulkas, M. Zahouily, E. Bilal *et al.*, *Int. J. Biol. Macromol.*, **96**, 340 (2017), <http://dx.doi.org/10.1016/j.ijbiomac.2016.12.040>
- ²⁵ V. Hospodarova, E. Singovszka and N. Stevulova, *Am. J. Anal. Chem.*, **9**, 303 (2018), <https://doi.org/10.4236/ajac.2018.96023>
- ²⁶ C. Huang, N. Hao, S. Bhagia, M. Li, X. Meng *et al.*, *Materialia*, **4**, 237 (2018), <https://doi.org/10.1016/j.mtl.2018.09.008>
- ²⁷ P. L. Bhutiya, N. Misra, M. Abdul Rasheed and S. Zaheer Hasan, *Int. J. Biol. Macromol.*, **117**, 435 (2018), <https://doi.org/10.1016/j.ijbiomac.2018.05.210>
- ²⁸ A. Ait Benhamou, *Cellulose*, **28**, 4625 (2021), <https://doi.org/10.1007/s10570-021-03842-6>
- ²⁹ E. Durmaz and S. Ateş, *Cellulose Chem. Technol.*, **55**, 755 (2021), <https://doi.org/10.35812/CelluloseChemTechnol.2021.55.63>
- ³⁰ E. Hafemann, R. Battisti, D. Bresolin, C. Marangoni and R. A. F. Machado, *Waste Biomass Valor.*, **11**, 6595 (2020), <https://doi.org/10.1007/s12649-020-00937-2>
- ³¹ K. Kavkler and A. Demšar, *Spectrochim. Acta - Part A Mol. Biomol. Spectrosc.*, **78**, 740 (2011), <https://doi.org/10.1016/j.saa.2010.12.006>
- ³² K. Schenzel, S. Fischer and E. Brendler, *Cellulose*, **12**, 223 (2005), <https://doi.org/10.1007/s10570-004-3885-6>
- ³³ U. P. Agarwal, in “Handbook of Nanocellulose and Cellulose Nanocomposites”, edited by H. Kargarzadeh, I. Ahmad, S. Thomas and A. Dufresne, Wiley-VCH, 2017, vol. 1, p. 609, <https://doi.org/10.1002/9783527689972.ch18>
- ³⁴ U. P. Agarwal, R. Sabo, R. S. Reiner, C. M. Clemons and A. W. Rudie, *Appl. Spectrosc.*, **66**, 750 (2012), <https://doi.org/10.1366/11-06563>
- ³⁵ W. Li, R. Wang and S. Liu, *BioResources*, **6**, 4271 (2011), <https://doi.org/10.15376/biores.6.4.4271-4281>
- ³⁶ Y. Nishiyama, J. Sugiyama, H. Chanzy and P. Langan, *J. Am. Chem. Soc.*, **125**, 14300 (2003), <https://doi.org/10.1021/ja037055w>
- ³⁷ Q. Lu, L. Tang, F. Lin, S. Wang, Y. Chen *et al.*, *Cellulose*, **21**, 3497 (2014), <https://doi.org/10.1007/s10570-014-0376-2>
- ³⁸ A. Adeniyi, D. Gonzalez-Ortiz, C. Pochat-Bohatier, O. Oyewo, B. Sithole *et al.*, *Alexandria Eng. J.*, **59**, 4201 (2020), <https://doi.org/10.1016/j.aej.2020.07.025>
- ³⁹ C. Verma, M. Chhajed, P. Gupta, S. Roy and P. K. Maji, *Int. J. Biol. Macromol.*, **175**, 242 (2021), <https://doi.org/10.1016/j.ijbiomac.2021.02.038>
- ⁴⁰ E. Abraham, B. Deepa, L. A. Pothan, M. Jacob, S. Thomas *et al.*, *Carbohydr. Polym.*, **86**, 1468 (2011), <http://dx.doi.org/10.1016/j.carbpol.2011.06.034>
- ⁴¹ C. Trilokesh and K. B. Uppuluri, *Sci. Rep.*, **9**, 1 (2019), <http://dx.doi.org/10.1038/s41598-019-53412-x>
- ⁴² F. Luzi, D. Puglia, F. Sarasini, J. Tirillò, G. Maffei *et al.*, *Carbohydr. Polym.*, **209**, 328 (2019), <https://doi.org/10.1016/j.carbpol.2019.01.048>
- ⁴³ T. Gabriel, A. Belete, G. Hause, R. H. H. Neubert and T. Gebre-Mariam, *J. Polym. Environ.*, **29**, 2964 (2021), <https://doi.org/10.1007/s10924-021-02089-3>
- ⁴⁴ A. García, J. Labidi, M. N. Belgacem and J. Bras, *Cellulose*, **24**, 693 (2017), <https://doi.org/10.1007/s10570-016-1144-2>
- ⁴⁵ N. Pandi, S. H. Sonawane and K. Anand Kishore, *Ultrason. Sonochem.*, **70**, 105353 (2021), <https://doi.org/10.1016/j.ultsonch.2020.105353>

⁴⁶ T. Fattahi Meyabadi, F. Dadashian, G. Mir Mohamad Sadeghi and H. Ebrahimi Zanjani Asl, *Powder Technol.*, **261**, 232 (2014), <http://dx.doi.org/10.1016/j.powtec.2014.04.039>

⁴⁷ L. Xing, J. Gu, W. Zhang, D. Tu and C. Hu, *Carbohyd. Polym.*, **192**, 184 (2018), <https://doi.org/10.1016/j.carbpol.2018.03.042>

⁴⁸ J. Marett, A. Aning and E. J. Foster, *Ind. Crop. Prod.*, **109**, 869 (2017), <http://dx.doi.org/10.1016/j.indcrop.2017.09.039>

⁴⁹ A. L. S. Pereira, D. M. do Nascimento, M. de sá M. Souza Filho, J. P. S. Morais, N. F. Vasconcelos *et al.*, *Carbohyd. Polym.*, **112**, 165 (2014), <http://dx.doi.org/10.1016/j.carbpol.2014.05.090>